Florian Schlüter, Michaela Wilhelm, Kurosch Rezwan

Surfactant assisted syntheses of monolithic hybrid ceramics with hierarchical porosity

Journal Article as: peer-reviewed accepted version (Postprint)

DOI of this document*(secondary publication): 10.26092/elib/2444

Publication date of this document: 08/09/2023

* for better findability or for reliable citation

Recommended Citation (primary publication/Version of Record) incl. DOI:

Florian Schlüter, Michaela Wilhelm, Kurosch Rezwan,
Surfactant assisted syntheses of monolithic hybrid ceramics with hierarchical porosity,
Journal of the European Ceramic Society, Volume 35, Issue 11, 2015, Pages 2963-2972, ISSN 0955-2219,
https://doi.org/10.1016/j.jeurceramsoc.2015.03.034.

Surfactant assisted syntheses of monolithic hybrid ceramics with hierarchical porosity

Florian Schlüter, Michaela Wilhelm *, Kurosch Rezwan

University of Bremen, Advanced Ceramics, Am Biologischen Garten 2, IW3, Germany

Received 5 December 2014; received in revised form 23 March 2015; accepted 25 March 2015

Abstract

A surfactant assisted emulsion-based syntheses route is presented for obtaining organo-silica-based monolithic hybrid ceramics with a hierarchical pore size distribution and tailorable surface characteristics. Methyl polysiloxane (MK) and methyl-phenyl polysiloxane (H44) with varying mixing ratios are selected as precursors, cross-linked and subsequently pyrolyzed at 500 °C or 600 °C, respectively. By adjusting the oil/water ratio and by tailoring the surfactant concentration controlled micro and macropore distributions with mesoscopic cell windows are obtained. After pyrolysis, specific surface areas of up to 600 m^2/g are achieved. In addition, due to the distinguished pyrolysis decomposition behavior of MK and H44, the adjustment of the surface characteristics in terms of hydrophobicity or hydrophilicity is demonstrated. The presented surfactant assisted emulsion-based process is hence highly suitable for tailoring pore size distribution and surface characteristics at the same time. Both material properties are pivotal features for catalysis and gas separation applications.

Keywords: Hybrid ceramic; Surface characteristics; Porosity; Monolithic material; Emulsion

1. Introduction

Polymer derived ceramics (PDC) have been under research for many applications due to their advantages like low cost synthesis or versatile shaping possibilities. Polysiloxane based hierarchical materials with distinguished functional organic groups are considered as innovative materials and thus applications in many fields are expected, e.g. optics, membranes or sensors [1–4]. Hybrid ceramics are a special group of PDC materials [5]. Multi-functional hybrid ceramics can be obtained by pyrolysis of organic-inorganic polysiloxane precursors under an atmosphere of nitrogen. In dependence of the applied pyrolysis temperature hybrid ceramics (400–800 °C), amorphous SiOC ceramics (800–1200 °C) or crystalline SiC (>1200 °C) are generated. Due to a partial decomposition of the organic moieties at temperatures around 400–600 °C a pronounced microporosity evolves for hybrid ceramic materials resulting in high specific surface areas of 400–700 m^2/g. Further, properties of these materials are in between of those of a ceramic and a polymeric material. Hybrid ceramic materials are therefore called Ceramers [6]. In many applications, e.g. adsorbent materials or carrier materials for catalysis, materials with controllable surface characteristics in terms of hydrophobicity/hydrophilicity and porosity on different length scales (micro-/meso-/macro) are needed. These characteristics can be adjusted by using Ceramers with different pyrolysis temperatures, precursor compositions and reaction conditions [7–9]. Additionally, monoliths with a sufficient mechanical stability and adjustable porosity are required for potential applications like adsorbents, filters or functional catalysts.

High internal phase emulsions (HIPEs) are a promising class of emulsions for application in sol-gel processing. These emulsions are defined by an internal phase volume fraction higher than 74% of the total emulsion volume. The droplets of the internal phase can show polyhedral and/or polydisperse appearance. Those droplets are usually separated by a thin film of the continuous phase [2,3]. The first polymer foams prepared with HIPEs were published in the 1960s [10]. These so called poly(HIPEs) are materials prepared by polymerizing the continuous, the internal or both phases [2,3]. Polymerizing of the

* Corresponding author. Tel.: +49 421 218 64944; fax: +49 421 218 64932.
E-mail address: mwilhelm@uni-bremen.de (M. Wilhelm).

http://dx.doi.org/ 10.1016/j.jeurceramsoc.2015.03.034

continuous phase leads usually to the formation of porous materials and polymerization of the internal phase results usually in polymer latex [11]. One important aspect is the choice of surfactant in regard to prepare o/w or w/o emulsions (oil-in-water respectively water-in-oil emulsions). The Bancroft rule that states that the surfactant bearing the higher affinity with one phase will promote this phase as the continuous one [12]. Another important aspect is the hydrophilic–lipophilic balance, known as the HLB balance. This value explains the affinity of the surfactant to a hydrophobic or hydrophilic phase [13].

The HIPE process was rarely used with polysiloxanes as starting material [14–20]. After the first synthesis of macroporous silica monoliths in 1998 with a combination of an o/w emulsion and a sol-gel processing by Imhof and Pine [20], further developments were made by Backov et al. [15–19]. These authors were able to generate a silica based monolithic material with a hierarchically porosity which was labeled Si(HIPE). Firstly, these materials were generated by using tetraethyl orthosilicate (TEOS), dissolved in the continuous phase, as precursor. An increasing or decreasing of the micelle size was observed by tailoring the oil/water ratios and with that an adjustment of the macroscopic cell window size is possible for the Si(HIPE)s. With increasing oil volume fractions the macrocellular cell size diminished drastically [15,21].

Monolithic Si(HIPE)s were generated not only using (TEOS) as precursor but also together with up to 20 wt.% of some organic functionalized polysiloxanes, e.g. phenyltriethoxysilane, methyltriethoxysilane or N-(3-trimethoxysilylpropyl)pyrrol [16]. These sol–gel derived open-cell hybrid monoliths show macroscopic void spaces with accessible micro- and mesoporosities. The general macroscopic structures for the Si(HIPE)s resembles aggregated hollow spheres. Additionally, the monolithic materials with both good integrity and mechanical properties are achieved [16,17,22]. However, using higher concentration of R-Si(OEt)$_3$ than 20 wt.% leads to powders instead of monolithic materials. The authors labeled these kind of materials organo-Si(HIPE)s or R-Si(HIPE)s [16]. Beside the described direct incorporation of functional groups a post-synthesis functionalization of a TEOS based Si(HIPE) support is also possible [19].

However, Vakifahmetoglu et al. used methyl polysiloxane as precursor in different types of emulsions (w/o; o/w and w/o/w, not HIPE) and obtained after curing and pyrolysis SiOC ceramic foam monoliths or porous micron sized spherical beads. The influence of the surfactant on the characteristics of the SiOC ceramic foam was not investigated [14].

In this paper we report on the synthesis of monolithic emulsion based Ceramers with tailorable surface characteristics and pore size distribution using an emulsion based process with different oil/water ratios including HIPEs. By adjusting the oil/water ratio different morphologies of the macroscopic structure including mesocopic cell windows can be achieved. Due to the distinguished pyrolysis decomposition behavior of the precursor methyl polysiloxane (MK) and methyl-phenyl polysiloxane (H44) an adjustment of the surface characteristics in terms of hydrophobicity and hydrophilicity is possible. Additionally, high specific surface areas up to 600 m^2/g are obtained after pyrolysis. The removal of the surfactant during rinsing offers further possibilities to alter the surface characteristics as well as various specific surface areas. The influence of the emulsion type, the removal of the surfactant and the precursor composition on pore size distribution and surface characteristic will be discussed. Additionally, the influence of the surfactants on different material properties like surface characteristics and pore size distribution will be discussed in detail. These new materials will be denoted MEBC (monolithic emulsion based creamers).

2. Experimental

2.1. Preparation

Hierarchical monolithic hybrid ceramics were prepared from the oligomeric precursors methyl polysiloxane (Silres® MK, WackerChemie AG) and H44 methyl-phenyl polysiloxane (Silres® H44, WackerChemie AG) or combination of them for binary mixtures (Fig. 1 and Table 1). MK and/or H44 were dissolved in 4 mL dodecane (ABCR Dr. Braunagel GmbH & Co. KG) at 55 °C (MK containing samples) or 85 °C (MK/H44 containing samples) to generate a 12 M solution, which acts as internal phase later. The aqueous phase acts as continuous phase and the oily phase as internal phase by using the surfactant TTAB because of HLB value and the *Bancroft* rule. The continuous phase was prepared from tetradecyltrimethylammonium bromide (TTAB, ABCR Dr. Braunagel GmbH & Co. KG) (35 wt.%) in HCl (pH 0.5). To generate the different oil-in-water

Table 1
Prepared materials and their composition, process and pyrolysis parameters.

Material denotation	Ratio of H44/MK [wt.%]	Oil/water ratio [vol.%]	Water rinsing [h]	Pyrolysis temperature [°C] (-*xxx*)
Part A				
MK-74-0-*xxx*[a]	0/100	74/26, HIPE	0	500/600
MK-60-0-*xxx*	0/100	60/40, MIPE	0	500/600
MK-50-0-*xxx*	0/100	50/50, MIPE	0	500/600
MK-40-0-*xxx*	0/100	40/60, MIPE	0	500/600
MK-26-0-*xxx*	0/100	26/74, LIPE	0	500/600
Part B				
MK-74-0-*xxx*	0/100	74/26, HIPE	0	500/600
MK-74-3-*xxx*	0/100	74/26, HIPE	3	500/600
MK-74-16-*xxx*	0/100	74/26, HIPE	16	500/600
MK-74-48-*xxx*	0/100	74/26, HIPE	48	500/600
MK-74-168-*xxx*	0/100	74/26, HIPE	168	500/600
Part C				
1.0-H44-74-0-*xxx*	100/0	74/26, HIPE	0	500/600
0.8-H44-74-0-*xxx*	80/20	74/26, HIPE	0	500/600
0.6-H44-74-0-*xxx*	60/40	74/26, HIPE	0	500/600
0.4-H44-74-0-*xxx*	40/60	74/26, HIPE	0	500/600
0.2-H44-74-0-*xxx*	20/80	74/26, HIPE	0	500/600
MK-74-0-*xxx*[a]	0/100	74/26, HIPE	0	500/600

[a] Same sample.

emulsions: I HIPE (internal phase volume > 74%), II LIPE (low internal phase emulsions, internal phase volume < 30%) [23] and III MIPE (medium internal phase volume, internal phase volume $30 < x < 74\%$) the phase with higher volume was added drop by drop under stirring (500 rpm) to the other phase. The reaction vessel was sealed and the emulsions were allowed to cross-linking for 5 days at room temperature, catalyzed by HCl. After two or three days, depending on the composition, a white monolithic solid will be formed from the emulsions. After decantation the samples were rinsed with water (10 mL, after 12 h the water was replaced with new one) for different times (Fig. 1 and Table 1) to remove the TTAB from the monolithic materials. To analyze that influence on the final characteristics different rinsing times are used after the first cross-linking step. This was followed by another drying and cross-linking step carried out in vacuum (~2 mbar) for 5 h at 150 °C. On the one hand the vacuum process at 150 °C allows the removal of *n*-dodecane and water, on the other hand a second thermal cross-linking step is performed at the same time to enhance the cross-linking degree. Subsequently the specimens were pyrolyzed at either 500 or 600 °C in an atmosphere of nitrogen. A heating rate of 120 °C/h was used up to 100 °C below the final temperature and then a heating of 30 °C/h were applied to avoid overheating. The specimens were pyrolyzed at the maximal temperature for 4 h. Instead of samples based on pure MK the H44 based samples are showing after pyrolysis a slightly yellow color which indicates already a higher decomposition at lower temperatures.

All materials investigated in this work and their composition, process and pyrolysis parameters are shown in Table 1. For samples based on pure MK the denotation is as follows: the used precursor, the oil/water ratio, the rinsing time with water in hours and the pyrolysis temperature in °C as *xxx*. The denotation of H44 containing samples is similar, but it begins with percentage of H44. To give an example, 0.8-H44-74-0-500 was prepared from H44 and MK in a ratio of 80:20 (wt.%) with an oil/water ratio of 74/26 (vol.%). No rinsing step was carried out for this sample and pyrolysis was done at 500 °C.

The sample set is divided in three parts: A, B and C. In part A different oil/water ratios for samples based on pure MK were used to analyze the influence of different emulsions on pore size distribution. The amount of oily internal phase was constant; the aqueous continuous phase was varied. In part B the effect of the surfactant TTAB on different characteristics was investigated in detail by using different rinsing times to remove TTAB from samples based on pure MK. In part C the dependency of oligomeric precursor on the characteristics was analyzed by using different ratios of H44 and MK with an oil/water ratio of 74/26 and without rinsing step.

2.2. Characterization

According to IUPAC notation, microporous materials have pore diameters of less than 2 nm (microscopic length scale) and macroporous materials have pore diameters of greater than

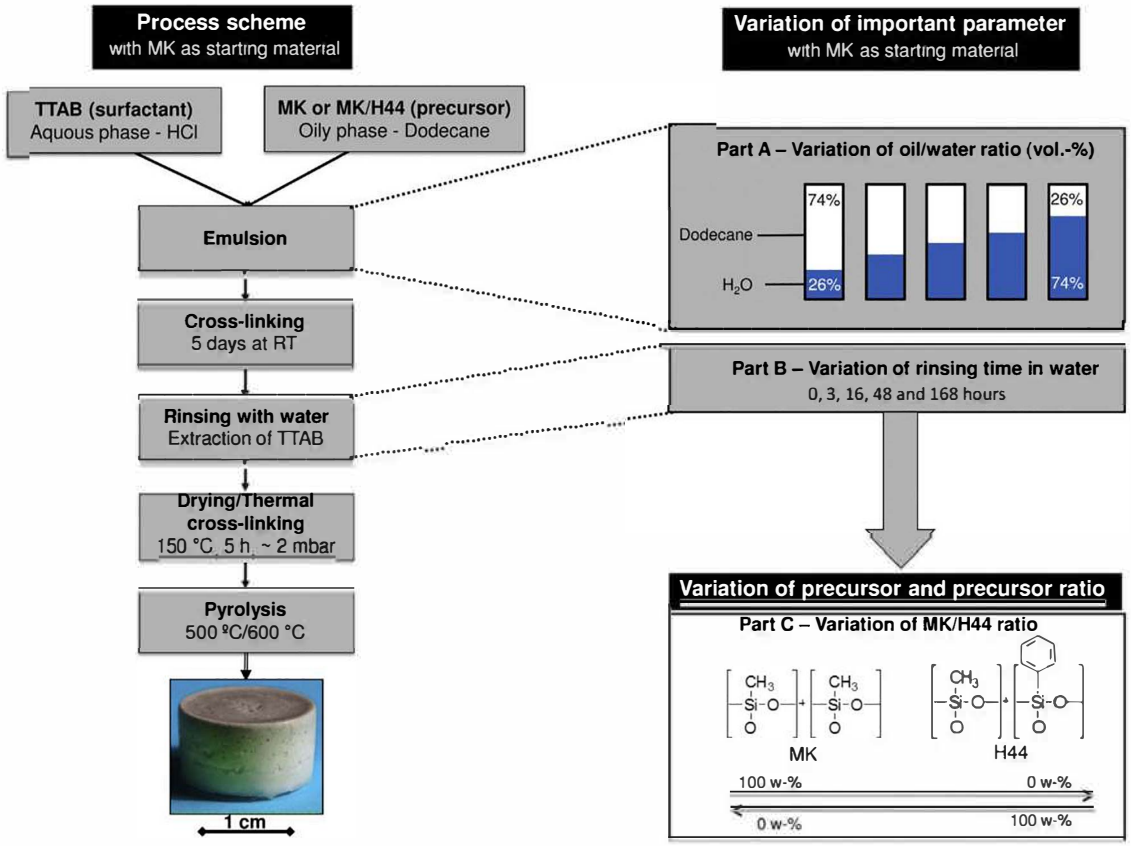

Fig. 1. Process scheme and parameter variation of synthesized samples: part A, samples based on pure MK with different oil/water ratios (74/26–26/74); part B, samples based on pure MK with an oil/water ratio of 74/26 with different rinsing times (0–168 h); part C, different ratios of H44 and MK (100–0 wt.% for H44) synthesized with an oil/water of 74/26 and without the rinsing step.

50 nm (macroscopic length scale). Mesoporous materials have pore diameter in a range from 2 to 50 nm (mesoscopic length scale) [24]. The macrostructure was analyzed from SEM images, which were recorded with 20 kV (Camscan Series 2, Obducat CamScan Ltd.) after embedding with two component epoxy resin, polishing with SiC paper and sputtering the specimens with gold (K550, Emitech, Judges Scientific plc.). Mercury intrusion was used to determine the macroporosity (Pascal 140/440 POROTEC GmbH) of the MEBC. The specific BET surface area was determined by nitrogen adsorption at −196 °C (Belsorp-Mini, Bel Japan Inc.) after grinding and sieving the material (mesh size 300 μm) to diminish limitation of nitrogen diffusion within the timeframe of the experiment. Moreover, the surface characteristics of these powder sieving fractions were investigated by isothermal water and *n*-heptane vapor sorption experiments at 22 °C, recording adsorption desorption isotherms (Belsorp18-3, Bel Japan Inc.).

3. Results

Preparation of monolithic emulsion based hybrid ceramics was done with silica precursor, which exhibits methyl and/or phenyl groups by using HIPEs, MIPEs or LIPEs. The introduction of organic groups was done with 100% polysiloxane precursors with the oligomers MK and H44 (for structures see Fig. 1) as precursors. The final monolith-type material is depicted in Fig. 1 and it shows for all samples sufficient handling stability.

3.1. Characterization at the macro and mesoscopic length scale

Using different oil/water ratios and with that HIPEs, MIPEs or LIPEs (materials of part A) macroscopic structures with variable morphologies can be achieved (Fig. 2, selected examples of the sample set).

For an oil/water ratio of 26/74 (Fig. 2a and b, LIPEs) monoliths composed of randomly packed hollow spheres were received. Using HIPEs (Fig. 2c–j) spherical macropores with different sizes were generated. Another result from the analysis of SEM pictures (Fig. 2c–j) concerns the macroscopic pores which are not monodisperse in size but rather polydisperse dependent on oil/water ratio as well as precursor composition. Well distributed spherical macropores with an interconnected porosity can be observed for the use of HIPEs (MK-74-0-500 and MK-74-0-600 in Fig. 2c and d as well as MK-74-168-500 and MK-74-168-600 in Fig. 2e and f). It should be noted that a structure with the mostly homogenous ordering is achieved by using HIPEs and pure MK as precursor (Fig. 2c–f).

Different rinsing times (removal of TTAB, part B) result not in big differences of the macroscopic structure (Fig. 2c and d compared to Fig. 2e and f). It becomes apparent that for these two compositions smaller macropores are generated for samples pyrolyzed at 600 °C. With increasing H44 amount a higher content of bigger and smaller pore sizes was found (part C, 0.4-H44-74-0-500, 0.4-H44-74-0-600, 1.0-H44-74-0-500 and 1.0-H44-74-0-600). Macropores up to 1000 μm can be generated by using only H44 as precursor (Fig. 2j).

The macroscopic morphology of the not pyrolyzed samples was investigated by SEM analysis too (not shown). This morphology shows the same macroscopic texture like the pyrolyzed samples. Thus, the formation of macropores is based on the emulsification process and not related to the pyrolysis. Additionally, it was possible to identify TTAB particles crystallized in the structure during drying containing bromide by EDX for the unwashed and not pyrolyzed samples (not shown).

Beyond SEM analysis mercury porosimetry was done to characterize more details of the macro- and mesoporosity. At first it should be mentioned that mercury porosimetry provides information only on the size of windows that connect two adjacent macropores, not the macropore diameters themselves. In Fig. 3a–d the accumulated volume and the relative pore volume versus pore diameter distribution of some examples of the sample set for different parts of this work (A, B and C) are depicted.

In Fig. 3a and b the meso- and macropore size distributions for samples with different oil/water ratios and pyrolysis temperatures are shown (part A). An adjustment of macropore sizes is possible for samples based on pure MK by using different oil/water ratios. HIPE materials (MK-74-0-500 and MK-74-0-600) show the smallest cell windows. Spherical macropores with cell windows are also observed in SEM pictures (Fig. 2). The diameter of the cell windows decreases with increasing pyrolysis temperature; for MK-74-0-500 the maximum diameter is around 0.4 μm and for MK-74-0-600 around 0.07 μm. The generation of smaller cell windows in the size between 0.002 and 0.05 μm (mesoporous) is possible for MEBC based on pure MK by using higher pyrolysis temperatures (Fig. 3b).

The pore size distribution of samples based on pure MK which were washed for different times with water and finally pyrolyzed at 500 °C are shown in Fig. 3c. The big influence of the rinsing time on the macroscopic structure is demonstrated by increasing sizes of the cell windows with longer rinsing times and thus enforced removal of TTAB. Starting from an average cell window size of 0.4 μm for the unwashed sample (MK-74-0-500, Fig. 3a) the cell window size increase to 0.8 μm after 3 h of rinsing for MK-74-3-500. Using longer rinsing times the shift of the average cell window size becomes more and more obvious. For MK-74-48-500 the average cell window size can be detected to be 40 μm. Rinsing for one week (MK-74-168-500) results in a broad pore size distribution where the big average cell window size (>100 μm) cannot be detected by this method. However, the SEM analysis shows macropores up to 400 μm (Fig. 2i and j). In Fig. 3d the pore size distribution of different compositions of the precursor pyrolyzed at 600 °C are depicted. Not only TTAB or the removal of TTAB can be used as structuring method; also the choice of the precursor can be used to tailor the macroscopic structure of the MEBC. To analyze the influence of the precursor composition only HIPE systems were investigated in order to tailor the surface characteristic and the pore size distribution. For materials made of MK only broad pore size distributions or a monomodal distribution are observed. In contrast, H44 and MK/H44 containing samples possess bimodal distribution of

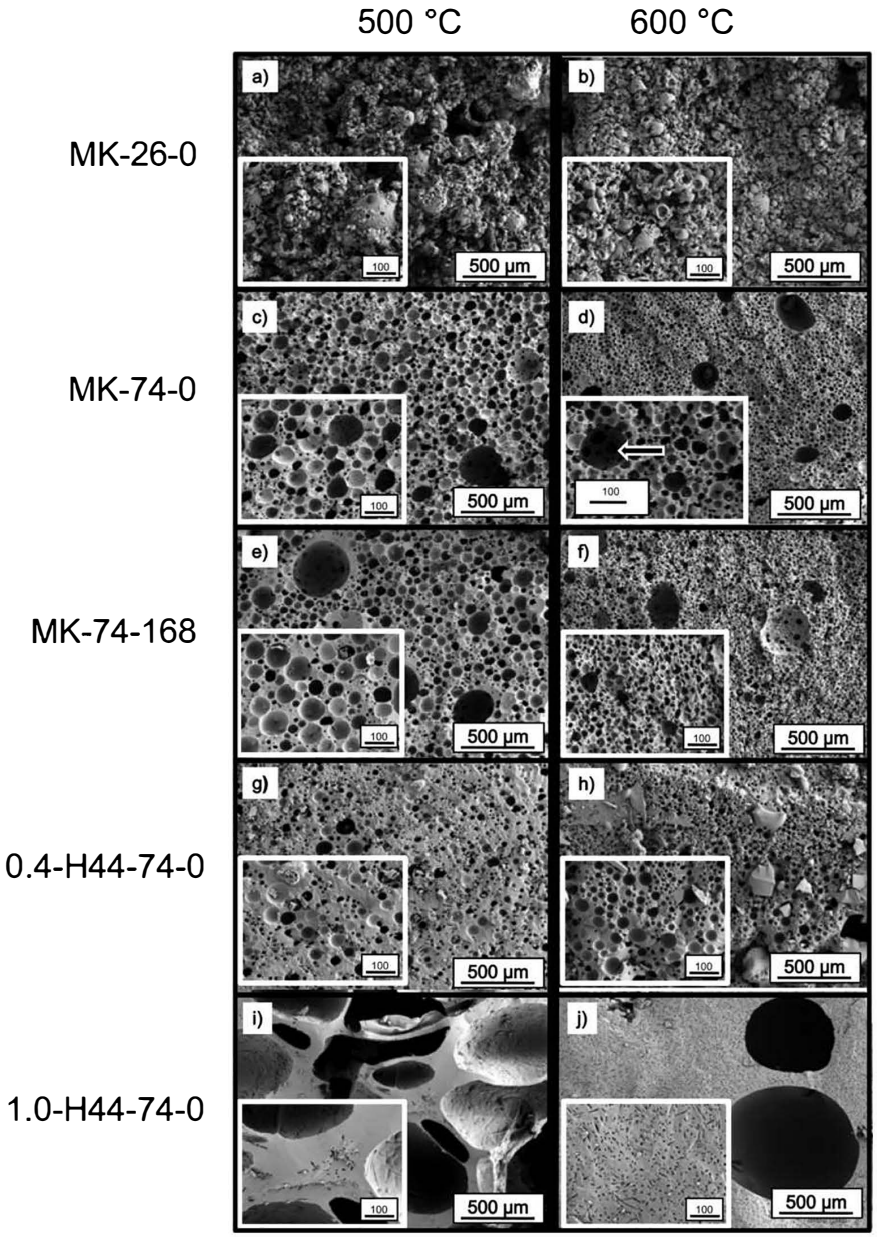

Fig. 2. SEM images of pyrolyzed monoliths with different oil/water ratios, rinsing times and MK/H44 ratios.

cell window sizes. For 0.6-H44-74-0-600 two separate peaks around 0.004 µm and around 100 µm are observed. One average cell window size of the H44 containing sample (1.0-H44-74-0-600) is located around 1.0 µm, the second average cell size expected from SEM cannot be detected by this method (detection limit 4 nm–120 µm). This is in agreement with the SEM pictures (Fig. 2i and j), which demonstrated already that many small but also very big macropores (up to 1000 µm) were generated.

3.2. Characterization at the microscopic length scale

Microporosity is important for realizing high specific surface areas that are available, e.g. for adsorption of gases and vapors or educts in catalytic applications. Micropores were investigated by nitrogen adsorption/desorption measurements and resulting isotherms as shown in Fig. 4a. Type I isotherms are characteristic for microporous materials [25]. All MEBC prepared in this study exhibit type I isotherms after pyrolysis indicating the pronounced microporosity of the materials. The specific BET surface areas (SSA) calculated from the nitrogen adsorption isotherms for the different parts (A, B and C) are shown in Fig. 4b–d. Microporosity was generated during pyrolysis for all kinds of materials at 500 and 600 °C. Further investigation of the not pyrolyzed materials (not shown here) indicates very low SSA areas around 5–30 m^2/g. It becomes clear, that the pyrolyzing steps are very important to generate high SSA. As already mentioned in the SEM part, the macroscopic morphology of the not pyrolyzed samples and the pyrolyzed samples are identical. In general it can be observed that the MEBC pyrolyzed at 600 °C generates higher SSA than the samples pyrolyzed at 500 °C. The explanation for that is the higher decomposition degree at 600 °C

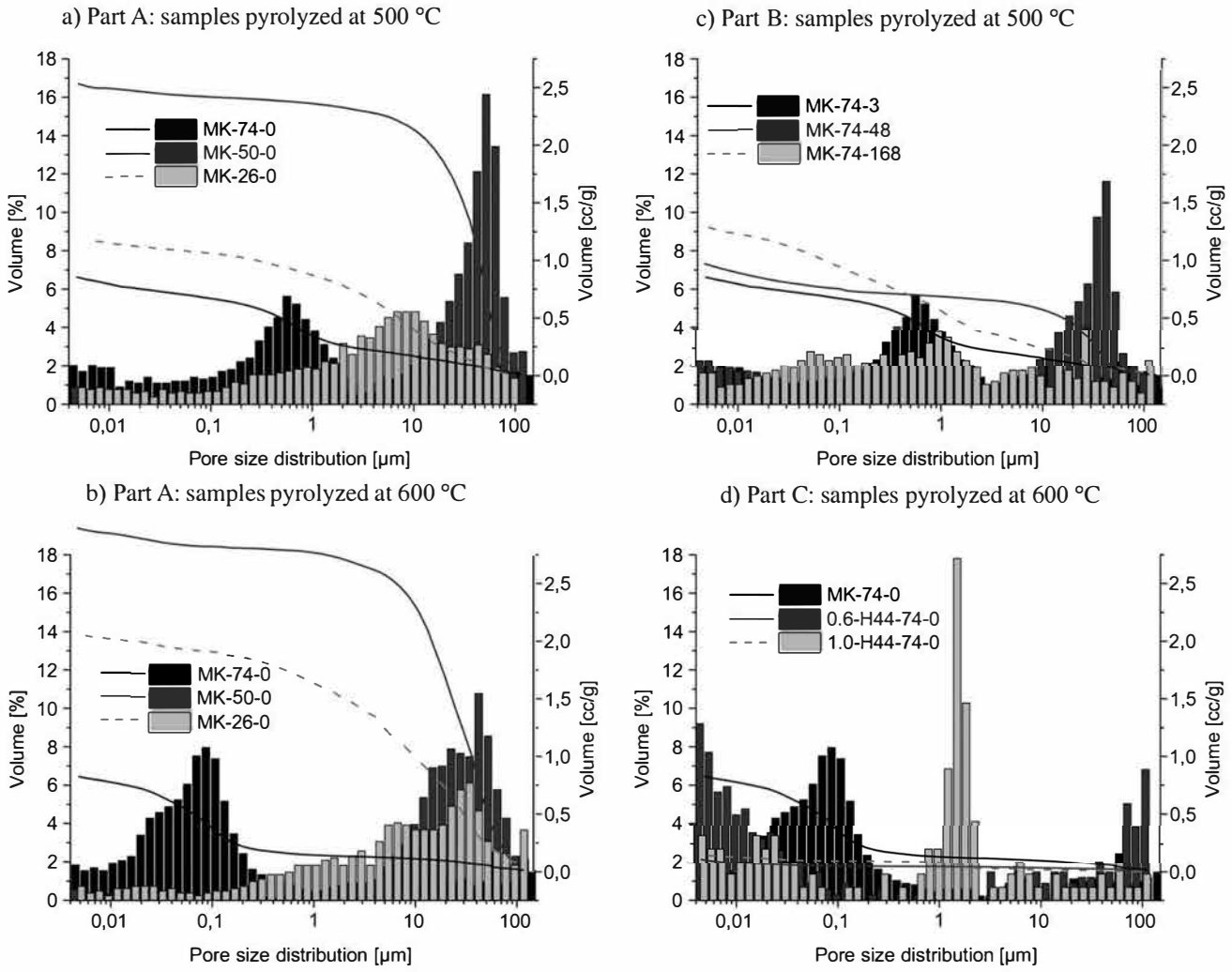

Fig. 3. Pore size distribution versus relative pore volume curves obtained from Hg-porosimetry of pyrolyzed samples: (a and b) with different oil/water ratios, (c) with different rinsing times pyrolyzed at 500 °C and (d) with different H44/MK ratios pyrolyzed at 600 °C.

which results in more micropores and in this way in higher SSA [7–9,26,27].

Fig. 4b demonstrates the dependency of SSA on the different emulsion types for samples based on pure MK (part A) pyrolyzed at 500 °C. The highest SSAs are generated for samples pyrolyzed at 600 °C (~380 m^2/g), while different types of emulsions do not affect the SSA of samples pyrolyzed at this temperature significantly. Additionally, the SSA for MEBC based on pure MK is comparable to MK containing samples, which were cross-linked under reflux and pyrolyzed at 600 °C (SSA: 360 m^2/g) [6,7]. The different emulsion types influence the SSA only for samples pyrolyzed at 500 °C (Fig. 4b). MK-74-0-500 has the highest surface area and with decreasing oil amounts a decreasing of the SSA is observed. The difference of the SSA for samples pyrolyzed at different temperature becomes much bigger for samples from part B (different rinsing times). For samples pyrolyzed at 600 °C only a weak effect of the rinsing time on the SSA is observed (Fig. 4c), because the SSA is mainly generated by the decomposition of MK. A further increase of the SSA by decomposition of TTAB is not possible at 600 °C. In contrast, a strong effect on the SSA for samples pyrolyzed at 500 °C due to the removal of TTAB is detected. Samples based on pure MK show at pyrolysis temperatures of 500 °C a low SSA. With increasing rinsing time a decrease of the SSA is observed.

Another tool to tailor the SSA is the precursor composition (part C, Fig. 4d). With increasing H44 content an increasing of the SSA is detected, while the only exceptions are MK-74-0-500 and MK-74-0-600. The reason for this might be that the surfactant TTAB is very well integrated in the cross-linked pure MK matrix and in this way, additional micropores can be generated during the pyrolysis process.

3.3. *Surface characteristics*

The surface characteristics of materials are important for interactions with, e.g. adsorbates or educts in catalysis application. The maximum adsorption of solvent vapors of different polarity at 22 °C was used in order to characterize the surface of the MEBC, as shown in Fig. 5 for selected materials. The solvents water and *n*-heptane are used as polar and nonpolar benchmark, respectively [28]. The uptakes are refered to the

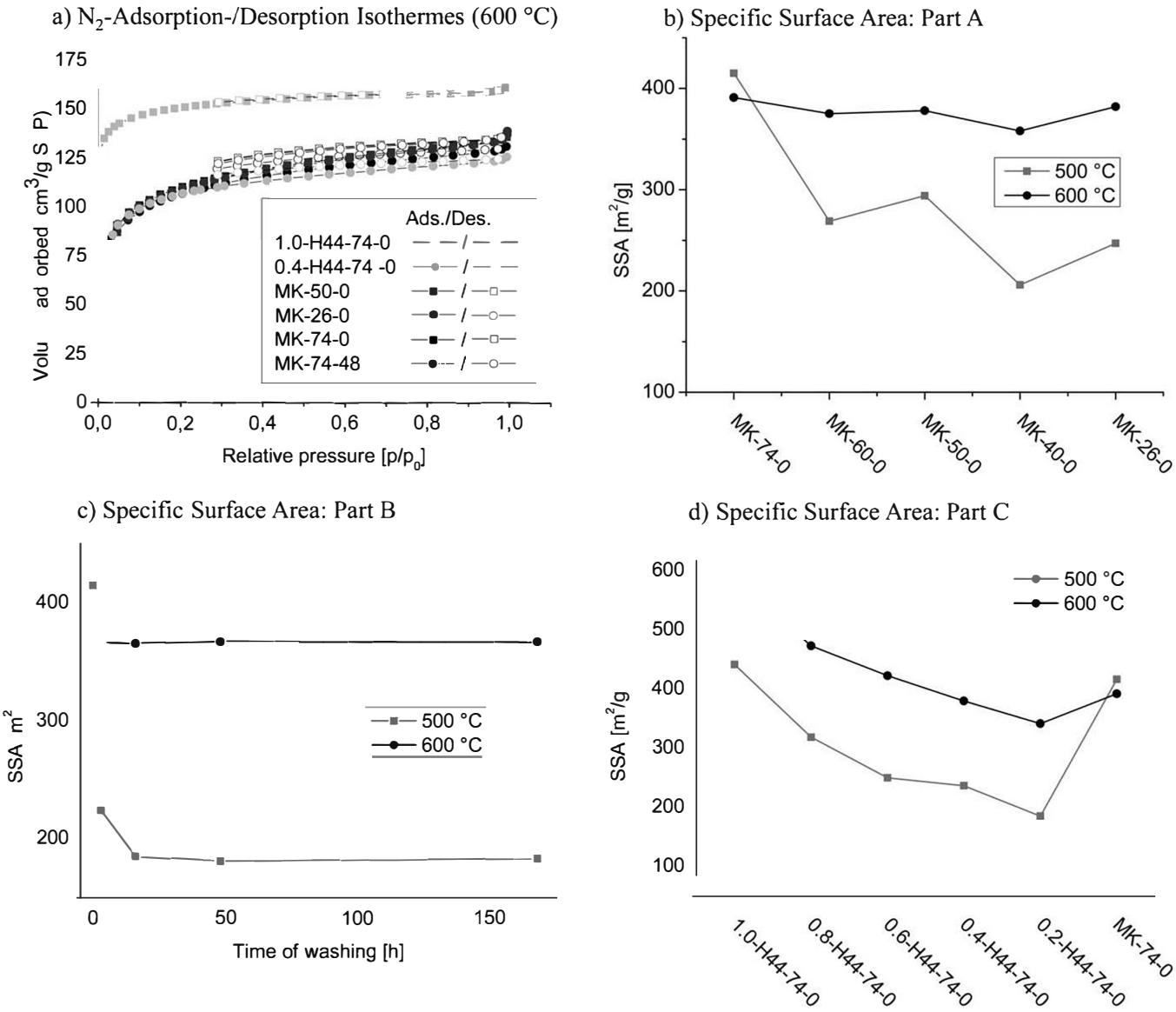

Fig. 4. (a) Nitrogen isotherms for different materials pyrolyzed at 600 °C and specific BET surface areas of pyrolyzed (500/600 °C) monoliths as determined by nitrogen adsorption with (b) different oil/water ratios; (c) different rinsing times; (d) different H44/MK ratios.

SSA gained from N_2 adsorption (Fig. 4). In Fig. 5a the results are shown for samples pyrolyzed at 500 °C and in Fig. 5b for samples pyrolyzed at 600 °C.

All samples generally adsorb more *n*-heptane vapor than water vapor, so that the analyzed MEBC have a higher affinity to nonpolar vapors. Using different emulsion types (part A, in Fig. 5a and b on the left side) a tailoring of the surface characteristics is not possible yet. For these materials the final composition of the pyrolyzed materials is the same, only the porosity on different length scales can be altered. Therefore, a constant *n*-heptane and water vapor adsorption are observed for samples pyrolyzed at 600 °C (Fig. 5b), which possess the same values of SSA too (Fig. 4b). There is no clear tendency for samples pyrolyzed at 500 °C. The varying uptake can be explained by the different SSA for samples pyrolyzed at 500 °C (Fig. 4b).

Samples, which belong to part B (different rinsing times) are shown centered in Fig. 5a and b. For samples pyrolyzed at 500 °C an influence of the rinsing time is observed. With increasing rinsing time a higher uptake of *n*-heptane is achieved. This effect is not observed for samples pyrolyzed at 600 °C. A constant vapor adsorption of *n*-heptane and water is observed. As discussed before, the influence of the surfactant TTAB affects the SSA of the samples pyrolyzed at 500 °C stronger than at 600 °C and with that different uptakes of water and *n*-heptane can be obtained.

A strong dependence of the surface characteristic is observed for part C. Different precursor compositions lead to different uptakes of water and *n*-heptane vapor for samples pyrolyzed at 600 °C (Fig. 5b, right side). A decreasing water vapor adsorption with increasing MK content is observed.

In summary, the decision to use the maximum adsorption capacities of water and *n*-heptane as boundary values allows comparing materials regarding their polar and dispersive interaction with vapors. Not only pore sizes and pore size distribution

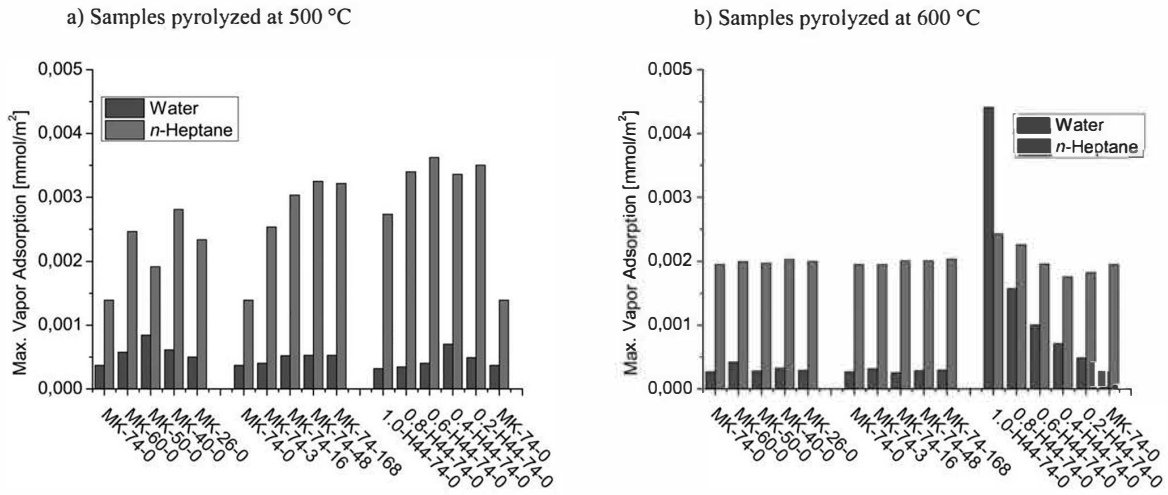

Fig. 5. Maximum n-heptane and water vapor adsorption and desorption at 22 °C with different oil/water ratios, different rinsing times and different ratios of H44/MK. (a) Samples pyrolyzed at 500 °C; (b) samples pyrolyzed at 600 °C. The sorption data were recalculated using the specific BET surface area from N_2 adsorption Fig. 4).

can be tailored by using the emulsion types HIPEs, MIPEs and LIPEs (part A), different rinsing times (part B) and different precursor composition (part C), but also the surface characteristic in terms of hydrophobicity/hydrophilicity can be tailored mainly by varying the precursor composition.

4. Discussion

Several characteristics like pore size distribution, SSA and surface characteristics in terms of hydrophobicity/hydrophilicity of the presented MEBC can be specifically tailored. An adjustment of pore size distribution by using different types of emulsions (HIPEs, MIPEs or LIPEs) or by selection of precursor is easy to achieve. The SSA and surface characteristics can be tailored by using different pyrolysis conditions or by selection of precursor, too. The use of the surfactant TTAB as a structuring agent affects all investigated properties like the pore size distribution, the SSA and surface characteristic of the MEBC. By this, the graded removal of TTAB by different rinsing times is a quick and easy to handle tool to adjust a set of properties at the same time. Those described properties and characteristics of MEBC are important for potential applications like carrier materials for catalysis and gas separation.

4.1. Tailoring of macro and mesostructure

Materials based on LIPE process (MK-26-0-500 and MK-26-0-600) show the morphology of randomly packed hollow spheres (Fig. 2a and b). Using LIPEs the internal oily phase has an amount of only 26 vol.%, so that oil droplets probably do not come in touch to each other. Cross-linking of the polysiloxane MK starts at the oil/water interface and extends to the inner core of the oil droplet, which might be explain the building of aggregated hollow spheres [15,16]. For materials based on the HIPE process well distributed spherical pores with an interconnected porosity are observed. Due to the high amount of the oily internal phase (74 vol.%) the oil droplets might only be separated by a very thin continuous phase at the beginning. The cross-linking should start again at the oil/water interface but due to the very thin water layers in between the chemical reaction proceeds as well to other oil droplets what results in a network with spherical pores. With increasing H44 content a higher content of bigger and smaller pore sizes were observed (Fig. 2g–j). A reason for that might be the different cross-linking behavior of MK and H44. It is also known, that different precursor results in different phase separation processes and surface tensions of the emulsions, which might explain the different macroscopic textures of the samples [3].

An important point at that stage is that the macroscopic texture of the pyrolyzed samples and the not pyrolyzed samples show the same morphology. Thus, the formation of macropores is based only on the emulsification process and is not related to the pyrolysis.

The results of the Mercury porosimetry support the SEM analysis. The pore size distribution can be tailored. By using structuring tools of different emulsion types, precursor selection and surfactant assisted synthesis an adjustment on the meso and macroscopic length scale is possible. By using different types of emulsions, for example LIPEs (MK-26-0-500 and MK-26-0-600) a broad pore size distribution is obtained, while the detected pores exhibit no cell windows in this case, but pores in between the cross-linked microbeads (Fig. 3a and b). The low ordering of the microbeads is responsible for the broad pore size distribution.

A reason for increasing pore sizes with increasing rinsing times for the MK-74-x samples might be that TTAB is incorporated in the polysiloxane matrix and during the rinsing step with water not only TTAB is removed from the monolith but also some fragments of the polysiloxane matrix (Fig. 3c). Consequently, it is possible to create bigger pores by using this surfactant assistant structuring method.

Mesocopic cell windows in the spherical pores can be observed as indicated in Fig. 2d with the arrow and Fig. 3a–d (Mercury porosimetry). There is still a discussion within the literature regarding the formation of the interconnected

cell windows [2]. Menner and Bismarck proposed that the interconnecting cell windows form after polymerization due to rinsing and drying processes [29]. In contrast to that, Cameron et al. proposed that these interconnecting cell windows are formed during polymerization due to density differences between polymer gel phase and the according phase of the emulsion and with that ruptures in the polymer film will be created [30]. This hypothesis is underlined from Krajnc et al. who observed interconnecting cell windows without rinsing and drying steps [31]. The macroscopic morphology of the new MEBC samples, which were not pyrolyzed, show also cell windows without any rinsing and drying steps (SEM pictures, not shown). Our observations are in agreement with Cameron et al. and Krajnc et al.

4.2. Tailoring of microstructure

As already mentioned above, the macroscopic morphology is independent of the pyrolysis. However, to generate high SSA for MK or H44 based materials it is necessary to use pyrolysis temperatures of 500 or 600 °C. Varying the pyrolysis temperature leads to different high SSAs and can be used as easy method to control the microporosity. Generally the MEBC pyrolyzed at 600 °C generates higher SSA than the samples pyrolyzed at 500 °C (Fig. 4b–d). The explanation for that is quite simple. MK and H44 show a higher decomposition degree at 500 °C compared to 600 °C, which results in a higher amount of micropores and by this in higher SSA [7–9,26,27].

Another tool to tailor the SSA is the variation of the rinsing time. With increasing rinsing time a decrease of the SSA is observed (Fig. 4c). The decomposition of TTAB creates micropores too, which explains the high SSA for the untreated samples based on pure MK. Previous works demonstrates that pure MK based samples, which were cross-linked under reflux and pyrolyzed at 500 °C show a SSA around 100 m^2/g [6]. From this it follows that the relative high SSA for samples pyrolyzed at 500 °C is mainly generated by the decomposition of TTAB. The surfactant assistant structuring method allows not only the tailoring of the macro and mesostructure but also the tailoring of microporosity and the resulting SSA.

As shown in Fig. 4d an increasing specific SSA with increasing H44 content is observed. It is known from previous works that H44 based materials generate more micropores than materials based on pure MK for pyrolysis temperature of 500 or 600 °C [26]. The resulting SSA is higher in the case of H44 than for MK since the phenyl groups decompose at lower temperatures of about 600 °C than the methyl groups. The same observations are confirmed for MEBC. The highest SSA (~600 m^2/g) is observed for 1.0-H44-74-0-600.

4.3. Surface characteristics

With increasing rinsing time a higher uptake of *n*-heptane is achieved (Fig. 5a). The removal of the ionic TTAB by rinsing and the remaining of less ionic parts in the pyrolyzed materials with longer rinsing times could explain this result. Also, a decreasing water vapor adsorption with increasing MK content is observed (Fig. 5b). The reason is that H44 shows a higher degree of decomposition compared to MK at a pyrolysis temperature of 600 °C. In this way a higher content of SiO_2 domains in the final material is generated [26] and so a higher affinity to water is achieved for 1.0-H44-74-0-600. Samples pyrolyzed at 500 °C (Fig. 5a, right side) with higher contents of H44 possess the most hydrophobic properties because the organic groups remain in the MEBC at these relatively low pyrolysis temperatures.

MEBC synthesized with silica precursor, which exhibits methyl and/or phenyl groups show a tailorable pore size distribution by using different emulsion types. Compared to Si(HIPE) [15–19] and R-Si(HIPE) [16,17,19,22] an introduction of organic groups to 100% and the generation of monolithic structures at the same time is possible. With that, an adjustment of surface characteristic in terms of hydrophobicity/hydrophilicity and generation of high SSA is manageable. Those properties make the new material suitable for new applications like catalysis and gas separation processes.

5. Conclusions

Monolithic emulsion based ceramers with hierarchical porosity were obtained by using a HIPE, MIPE or LIPE processes, starting with silica precursor, which exhibits only methyl and/or phenyl groups (MK and H44). The resulting compounds which were denoted monolithic emulsion based Ceramers (MEBC) were analyzed in detail in terms of porosity and surface characteristics. Tailoring of macroscopic structure is possible by using different kinds of emulsions (HIPEs, MIPEs or LIPEs). Depending on the emulsion type it is possible to generate monoliths composed of either microbeads or spherical pores with cell window sizes in the meso and microscopic range. Additionally, controllable micro and macropore distributions with mesoscopic cell windows are obtained. Tailoring of the surface characteristics in terms of hydrophobicity/hydrophilicity is possible by precursor selection, using a methyl and phenyl group containing precursor (H44) or a precursor with only methyl (MK) groups in different ratios. The pyrolysis of different precursor composition at 500 or 600 °C results in specific BET surface areas up to 600 m^2/g without losing the monolithic structure.

The use of the surfactant TTAB as a structuring agent leads to tailorable macro and microporosity with cell window sizes in a mesoscopic length scale, and also tailoring of the surface characteristic in terms of hydrophobicity/hydrophilicity is achievable.

These materials feature a sufficient handling stability and high specific BET surface areas, which make this material highly suitable for applications like support materials for catalysis or adsorbent materials.

Acknowledgements

This work was supported by the German Research Foundation (DFG) within the Research Training Group 1860 "Micro-, meso- and macroporous nonmetallic Materials: Fundamentals and Applications". Alonso Menezes de Oliveira Junior is gratefully acknowledged for his preliminary work in the laboratory.

References

[1] Cameron NR. High internal phase emulsion templating as a route to well-defined porous polymers. Polymer 2005;46:1439–49.

[2] Pulko I, Krajnc P. High internal phase emulsion templating – a path to hierarchically porous functional polymers. Macromol Rapid Commun 2012;33:1731–46.

[3] Triantafillidis C, Elsaesser MS, Hüsing N. Chemical phase separation strategies towards silica monoliths with hierarchical porosity. Chem Soc Rev 2013;42:3833–46.

[4] Silverstein MS. Emulsion-templated porous polymers: a retrospective perspective. Polymer 2014;55:304–20.

[5] Terauds K, Sanchez-Jimenez PE, Raj R, Vakifahmetoglu C, Colombo P. Giant piezoresistivity of polymer-derived ceramics at high temperatures. J Eur Ceram Soc 2010;30:2203–7.

[6] Prenzel T, Guedes TLM, Schlüter F, Wilhelm M, Rezwan K. Tuning surfaces of hybrid ceramics for gas adsorption – from alkanes to CO_2. Sep Purif Technol 2014;129:80–9.

[7] Prenzel T, Wilhelm M, Rezwan K. Pyrolyzed polysiloxane membranes with tailorable hydrophobicity, porosity and high specific surface area. Microporous Mesoporous Mater 2013;169:160–7.

[8] Adam M, Wilhelm M, Grathwohl G. Polysiloxane derived hybrid ceramics with nanodispersed Pt. Microporous Mesoporous Mater 2012;151:195–200.

[9] Wilhelm M, Soltmann C, Koch D, Grathwohl G. Ceramers – functional materials for adsorption techniques. J Eur Ceram Soc 2005;25:271–6.

[10] von Bonin W, Bartel H. Polymerization of vinyl compounds in water-in-oil emulsions, (Farbenfabriken Bayer A.-G.). Application: DE, 4; 1962.

[11] Zhang H, Cooper AI. Synthesis and applications of emulsion-templated porous materials. Soft Matter 2005;1:107–13.

[12] Bancroft WD. J Phys Chem 1913;17:501–20.

[13] Griffin WJ. Classification of surface-active agents by HLB. J Soc Cosmet Chem 1949;1:311–21.

[14] Vakifahmetoglu C, Balliana M, Colombo P. Ceramic foams and microbeads from emulsions of a preceramic polymer. J Eur Ceram Soc 2011;31:1481–90.

[15] Carn F, Colin A, Achard MF, Deleuze H, Sellier E, Birot M, et al. Inorganic monoliths hierarchically textured via concentrated direct emulsion and micellar templates. J Mater Chem 2004;14:1370–6.

[16] Ungureanu S, Birot M, Laurent G, Deleuze H, Babot O, Julian-Lopez B, et al. One-Pot syntheses of the first series of emulsion based hierarchical hybrid organic-inorganic open-cell monoliths possessing tunable functionality (Organo-Si(HIPE) Series). Chem Mater 2007;19:5786–96.

[17] Ungureanu S, Deleuze H, Sanchez C, Popa MI, Backov R. First Pd@Organo-Si(HIPE) open-cell hybrid monoliths generation offering cycling Heck catalysis reactions. Chem Mater 2008;20:6494–500.

[18] Brun N, Prabaharan SRS, Morcrette M, Sanchez C, Pecastaings G, Derre A, et al. Hard macrocellular silica Si(HIPE) foams templating micro/macroporous carbonaceous monoliths: applications as lithium ion battery negative electrodes and electrochemical capacitors. Adv Funct Mater 2009;19:3136–45.

[19] Ungureanu S, Laurent G, Deleuze H, Babot O, Achard MF, Popa MI, et al. Syntheses and characterization of new organically grafted silica foams. Colloids Surf A 2010;360:85–93.

[20] Imhof A, Pine DJ. Uniform macroporous ceramics and plastics by emulsion templating. Chem Eng Technol 1998;21:682–5.

[21] Carn F, Colin A, Achard MF, Deleuze H, Saadi Z, Backov R. Rational design of macrocellular silica scaffolds obtained by a tunable sol–gel foaming process. Adv Mater 2004;16:140–4.

[22] Brun N, Julian-Lopez B, Hesemann P, Laurent G, Deleuze H, Sanchez C, et al. Eu3 + @Organo-Si(HIPE) macro-mesocellular hybrid foams generation: syntheses, characterizations, and photonic properties. Chem Mater 2008;20:7117–29.

[23] Manley SS, Graeber N, Grof Z, Menner A, Hewitt GF, Stepanek F, et al. New insights into the relationship between internal phase level of emulsion templates and gas-liquid permeability of interconnected macroporous polymers. Soft Matter 2009;5:4780–7.

[24] Rouquerol J, Avnir D, Fairbridge CW, Everett DH, Haynes JH, Pernicone N, et al. Recommendations for the characterization of porous solids. Pure Appl Chem 1994;66:1739–58.

[25] Sing KSW, Everett DH, Haul RAW, Moscou L, Pierotti RA, Rouquerol J, et al. Reporting physisorption data for gas/solid systems with special reference to the determination of surface area and porosity (Recommendations 1984). Pure Appl Chem 1985;57:603–19.

[26] Scheffler M, Gambaryan-Roisman T, Takahashi T, Kaschta J, Muenstedt H, Buhler P, et al. Pyrolytic decomposition of preceramic organo polysiloxanes. Ceram Trans 2000;115:239–50.

[27] Wilhelm M, Adam M, Bäumer M, Grathwohl G. Synthesis and properties of porous hybrid materials containing metallic nanoparticles. Adv Eng Mater 2008;10:241–5.

[28] Stana-Kleinschek K, Ribitsch V, Kreze T, Fras L. Determination of the adsorption character of cellulose fibres using surface tension and surface charge. Mater Res Innov 2002;6:13–8.

[29] Menner A, Bismarck A. New evidence for the mechanism of the pore formation in polymerising high internal phase emulsions or why polyHIPEs have an interconnected pore network structure. Macromol Symp 2006;242:19–24.

[30] Cameron NR, Sherrington DC, Albiston L, Gregory DP. Study of the formation of the open-cellular morphology of poly(styrene/divinylbenzene) polyHIPE materials by cryo-SEM. Colloid Polym Sci 1996;274:592–5.

[31] Paljevac M, Jeřabek K, Krajnc P. Crosslinked poly(2-hydroxyethyl methacrylate) by emulsion templating: influence of crosslinker on microcellular structure. J Polym Environ 2012;20:1095–102.